Anomalous dynamic backaction in interferometers

Sergey P. Tarabrin,[1,2,*] Henning Kaufer,[1] Farid Ya. Khalili,[3] Roman Schnabel,[1] and Klemens Hammerer[1,2]

[1]*Institut für Gravitationsphysik, Leibniz Universität Hannover and Max-Planck-Institut für Gravitationsphysik (Albert-Einstein-Institut), Callinstraße 38, 30167 Hannover, Germany*

[2]*Institut für Theoretische Physik, Leibniz Universität Hannover, Appelstraße 2, 30167 Hannover, Germany*

[3]*Moscow State University, Department of Physics, Moscow 119992, Russia*

(Received 7 February 2013; published 6 August 2013)

We analyze the dynamic optomechanical backaction in signal-recycled Michelson and Michelson-Sagnac interferometers that are operated off the dark port. We show that in this case—and in contrast to the well-studied canonical form of dynamic backaction on the dark port—optical damping in a Michelson-Sagnac interferometer acquires a nonzero value on cavity resonance, and additional stability and instability regions on either side of the resonance, revealing additional regimes of cooling and heating of micromechanical oscillators. In a free-mass Michelson interferometer for a certain region of parameters we predict a stable single-carrier optical spring (positive spring *and* positive damping), which can be utilized for the reduction of quantum noise in future-generation gravitational-wave detectors.

DOI: 10.1103/PhysRevA.88.023809 PACS number(s): 42.50.Wk, 04.80.Nn, 07.10.Cm, 07.60.Ly

I. INTRODUCTION

It is a fundamental result of quantum measurement theory that in any optomechanical system, where light serves as a quantum readout agent interacting with a mechanical probe (test mass) via radiation pressure, the probe is subject to measurement *backaction* [1–5]. Already in the simplest setup comprised of a mirror in "free space" [see Fig. 1(a)], quantum fluctuations of the electromagnetic field exert *backaction noise* on the probe [6] which causes the standard quantum limit (SQL) of measurement precision [7–9]. This can become relevant in setups where the optical field is resonantly enhanced, as in a Fabry-Pérot (FP) cavity [see Fig. 1(d)]. In this way backaction noise has been observed very recently both directly [10,11] and indirectly via ponderomotive squeezing [12,13]. In addition, resonant field enhancement causes *dynamic backaction*: modulation of the intracavity field by the motion of the probe produces a ponderomotive force, which alters the dynamical properties of the probe, as was first recognized in [14,15]. Dynamic backaction comprises a shift of the probe's (i) intrinsic damping rate (*optical damping*), and (ii) mechanical frequency (*optical spring*). Both effects have been studied and observed in FP cavities (or equivalent systems) in a regime of *dispersive coupling* (motion of the probe modulates the cavity resonance frequency), and utilized for, respectively, optical backaction cooling [16,17] of micromechanical oscillators [18–28] and optical trapping of a gram-scale mirror [29,30].

In this paper we address dynamic backaction in standard two-path interferometers, such as, e.g., Michelson or Sagnac interferometers (cf. Fig. 1). High-precision measurements commonly employ such interferometric topologies because a path differential measurement in a balanced interferometer significantly suppresses path common noise, such as laser noise. The prime example is the Michelson topology of gravitational-wave detectors (GWDs). State-of-the-art balanced interferometers utilize resonant field enhancement techniques, similar to FP cavities [3,31]. For instance, an additional mirror positioned in the interferometer's input and/or output port, referred to as the power-recycling (PR) and the signal-recycling (SR) mirror, respectively, provides amplification of the laser power and/or the signal field [32]. Just as in a FP cavity, the resonant field amplification in recycled interferometers implies dynamic backaction on the test masses. So far, the associated optomechanical effects have been considered exclusively in interferometers perfectly tuned to a dark fringe (vanishing mean power) in the output port (hence, dark port). The operation on *or close to* the dark port is in fact the generic working point as it provides the most sensitive signal transduction [see Fig. 1(c)], and on top of this ensures that laser noise is rejected from the interferometer's output. On dark port the *scaling law* [33] provides a general framework for understanding the optomechanics of interferometers: it states that the dynamical and noise properties of any interferometer with high-finesse signal mode and operated on dark port are equivalent to the ones derived from the dispersive optomechanics of a FP cavity with corresponding effective linewidth, detuning, and circulating optical power. Here we show that the dynamic backaction in any SR interferometer operated *off dark port* exhibits rather surprising, anomalous features as compared to the canonical one in a FP cavity as derived within the scope of the scaling law.

We show this for the concrete setups of (i) a Michelson-Sagnac interferometer (MSI) with a semitransparent membrane [34,35] [see Fig. 1(f)], as relevant to the optomechanical experiments with micro- and nanomechanical test masses, and (ii) a free-mass Michelson interferometer (MI), as relevant to GWDs [see Fig. 1(e)]. We emphasize that our logic applies immediately to other interferometric topologies. In particular, we found that optical damping in a MSI as a function of detuning acquires a nonzero value on cavity resonance and additional cooling and heating regions on either side of the resonance. In a MI the optical spring and damping acquire intersecting regions of positive and negative values. This is of particular interest for free-mass GWDs as the intricate frequency dependence of the optical spring has been studied (within the scope of the scaling

*Corresponding author: sergey.tarabrin@aei.mpg.de

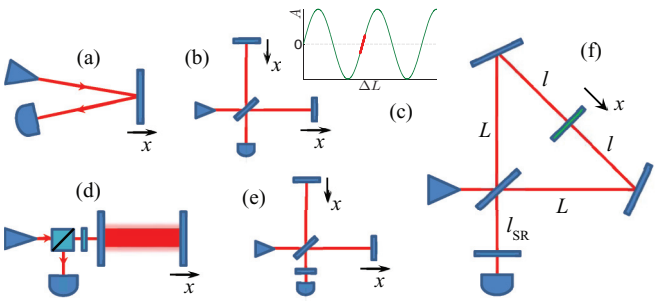

FIG. 1. (Color online) Optomechanical setups. (a) The simplest setup for measuring the position of the test mass (mirror) via a reflected laser beam. (b) A Michelson interferometer with end mirrors performing antisymmetric motion. (c) Field amplitude at the output port of a Michelson interferometer as a function of arm-length difference. Points of zero amplitude correspond to dark fringes in the interference pattern. In a small vicinity near the dark fringe (marked with thick red) linear signal transduction is possible. (d) Resonant amplification of the optical field in a Fabry-Pérot cavity. (e) A signal-recycled Michelson interferometer. (f) A signal-recycled Michelson-Sagnac interferometer with an oscillating semitransparent membrane.

law) as a means for increasing the sensitivity via tailoring the dynamics of the test masses [36–41].

From the viewpoint of cavity optomechanics the anomalous dynamic backaction can be understood as being caused by the emergence of *dissipative coupling* (motion of the test mass modulates the cavity linewidth) [42–47] and its interplay with the usual dispersive coupling. Recently some of the present authors showed that a specially tuned MSI can indeed exhibit a pure dissipative coupling [46]. Here we show that the anomalies in dynamic backaction have to be expected generically for any SR interferometer operated off dark port, even when no simple description in terms of dispersive and dissipative coupling is possible.[1]

II. CANONICAL AND ANOMALOUS DYNAMIC BACKACTION

We derive the dynamic backaction in a SR MSI (which covers the MI as a special case) using a transfer matrix approach to the propagation of fields in the frequency domain [3]. Details of the calculations are presented in Appendix A. First we characterize the nonrecycled MSI as an effective mirror whose reflectance ρ and transmittance τ depend on the position of the membrane $x = \delta l/2$, with δl being the imbalance of the interferometer arms [46]:

$$\rho = R_{\rm m}\left(T_{\rm BS}^2 e^{ik_0\delta l} - R_{\rm BS}^2 e^{-ik_0\delta l}\right) - 2T_{\rm m}R_{\rm BS}T_{\rm BS},$$
$$\tau = R_{\rm m}R_{\rm BS}T_{\rm BS}\left(e^{ik_0\delta l} + e^{-ik_0\delta l}\right) + T_{\rm m}\left(T_{\rm BS}^2 - R_{\rm BS}^2\right).$$

[1]The notions of dispersive and dissipative coupling, defined for instance in [42], being unambiguous for a single-mode optomechanical cavity, can become ambiguous for a multimode system. In particular, in a two-arm interferometer, which is a two-mode system, the type of coupling of the normal mode(s) to the test masses can be different from that of the partial mode(s).

Here $k_0 = \omega_0/c = 2\pi/\lambda_0$ is the laser carrier wave number, $R_{\rm BS} > 0$ and $T_{\rm BS} > 0$ are the amplitude reflectivity and transmissivity of the beam splitter, and $R_{\rm m} > 0$ and $T_{\rm m} > 0$ are the amplitude reflectivity and transmissivity of the membrane. The reflectance ρ describes reflection of the input vacuum field from the detector port, while $-\rho^*$ describes reflection of the input laser field. The dark port condition for the interferometer is achieved when $\tau = 0$, which is satisfied for $\delta l_{\rm DP} = n\lambda_0/4$ and odd n in the case of a balanced beam splitter, $R_{\rm BS} = T_{\rm BS} = 1/\sqrt{2}$.

Insertion of the SR mirror (SRM) of amplitude reflectivity $R_{\rm SR} > 0$ and transmissivity $T_{\rm SR} > 0$ effectively transforms an interferometer into a FP cavity whose second mirror is defined by the MSI. The inverse resonance factor of this effective cavity,

$$\mathcal{D} = 1 - R_{\rm SR}|\rho|e^{2ik_0\mathcal{L}+i\arg\rho} = 1 - R_{\rm SR}|\rho|e^{2i\Delta\mathcal{L}/c},$$

where $\mathcal{L} = L + l + l_{\rm SR}$ is the effective cavity length [the total length between the SRM and the membrane; see Fig. 1(f)], describes modulation of the cavity resonance frequency *and* linewidth by the motion of the membrane, featuring dispersive and dissipative couplings respectively [46]. In particular, the total detuning Δ of the laser carrier frequency ω_0 from the cavity resonance reads

$$\Delta = \delta_{\rm SR} + \delta_{\rm m}, \quad \delta_{\rm SR} = \omega_0 - \omega_{\rm cav}, \quad \delta_{\rm m} = \frac{c}{2\mathcal{L}}\delta\phi,$$
$$\omega_{\rm cav} = \frac{c}{\mathcal{L}}\pi N - \frac{c}{2\mathcal{L}}\arg\rho_{\rm DP}, \quad \delta\phi = \arg\rho - \arg\rho_{\rm DP}.$$

Here N is a fixed integer, $\rho_{\rm DP} = \rho(\delta l_{\rm DP})$, $\delta_{\rm SR}$ is the detuning from the cavity resonance $\omega_{\rm cav}$ at the dark port, defined by the position of the SRM, and $\delta_{\rm m}$ is the detuning due to offset from the dark port, defined by the position of the membrane, and hence describing the dispersive coupling in the effective cavity. Similarly, the total half-linewidth γ of the latter in the narrowband approximation ($T_{\rm SR} \ll 1$, $\tau \ll 1$),

$$\gamma = \frac{1 - R_{\rm SR}|\rho|}{2\mathcal{L}/c} = \gamma_{\rm SR} + \gamma_{\rm m}, \quad \gamma_{\rm SR} = \frac{cT_{\rm SR}^2}{4\mathcal{L}}, \quad \gamma_{\rm m} = \frac{c\tau^2}{4\mathcal{L}},$$

accounts for the finite transmittances of the SRM via $\gamma_{\rm SR}$, and of the MSI operated off dark port via $\gamma_{\rm m}$, the latter thus describing dissipative coupling in the effective cavity.

We then compute the fields incident on the membrane and derive the corresponding radiation pressure force, which consists of (i) the radiation pressure noise, which is a stochastic backaction due to vacuum fluctuations entering from the laser and detector ports, and (ii) the ponderomotive force due to motion of the membrane $x(\Omega)$. The unsymmetrized spectral density of backaction noise exhibits a mixture of Lorentz- and Fano-like resonances, the latter owing to the interference between input and intracavity laser fields (see Refs. [42,46] and Appendix B). The ponderomotive force $F_x(\Omega) = -\mathcal{K}(\Omega)x(\Omega)$, calculated in Appendix C, creates a dynamic backaction $\mathcal{K}(\Omega)$, comprised of the optical spring $K(\Omega) = {\rm Re}[\mathcal{K}(\Omega)]$ and optical damping $\Gamma(\Omega) = -\frac{1}{2}{\rm Im}[\mathcal{K}(\Omega)]/\Omega$, such that the corresponding shifts of the square of the mechanical frequency and mechanical damping rate are K/m and Γ/m, with m being the membrane's (effective) mass.

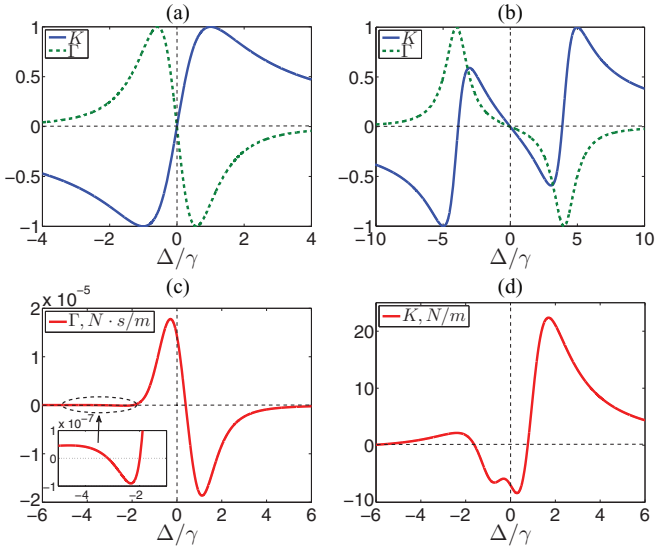

FIG. 2. (Color online) (a) Canonical K and Γ defined in Eq. (1) for $\xi = 0$, normalized to their respective maximum values, for $\Omega < \gamma$. (b) Same for $\Omega > \gamma$. (c) and (d) respectively show the optical damping and spring in the signal-recycled MSI detuned from the dark port at $\delta l_{\rm DP} = 3\lambda_0/4$ by $\xi \approx 0.01\lambda_0$, with $P_{\rm in} = 200$ mW, $\lambda_0 = 1064$ nm, $\mathcal{L} = 8.7$ cm, $R_{\rm m}^2 = 0.17$, $T_{\rm SR}^2 = 3 \times 10^{-4}$, and $\gamma \approx \Omega = 2\pi \times 133$ kHz.

We present the formula for $\mathcal{K}(\Omega)$, which is rather complicated in the general case, using the following simplifying assumptions: (i) a balanced beam splitter, (ii) a single optical mode with narrow linewidth $\gamma \ll c/\mathcal{L}$, and (iii) small displacements of the membrane from the position corresponding to the dark fringe, $\langle x \rangle = \xi/2 \ll \lambda_0$, with $\xi = \delta l - \delta l_{\rm DP}$. Under these conditions, $\gamma_{\rm m} = cR_{\rm m}^2(k_0\xi)^2/4\mathcal{L}$, $\delta_{\rm m} = \pm cR_{\rm m}T_{\rm m}(k_0\xi)^2/4\mathcal{L}$,[2] and the dynamic backaction reads

$$\mathcal{K}(\Omega) = \frac{4\omega_0 R_{\rm m}^2 P_{\rm in}}{c\mathcal{L}} \frac{1}{\Delta^2 + (\gamma - i\Omega)^2} \times \left\{ \frac{\delta_{\rm SR}[\gamma^2 + \Delta^2 - 4(\gamma\gamma_{\rm m} + \Delta\delta_{\rm m})]}{\gamma^2 + \Delta^2} + \frac{2i(\gamma_{\rm SR}\delta_{\rm m} + \gamma_{\rm m}\delta_{\rm SR})\Omega + \delta_{\rm m}\Omega^2}{\gamma^2 + \Delta^2} \right\}, \quad (1)$$

where $P_{\rm in}$ is the input laser power. For $\xi = 0$ (on the dark port) Eq. (1) reduces to the canonical spring and damping of a simple FP cavity with pure dispersive coupling [33,37]. These canonical K and Γ possess the following characteristic features: (i) Both are antisymmetric with respect to Δ and vanish at $\Delta = 0$, (ii) Γ as a function of Δ crosses zero only once, being positive for $\Delta < 0$ and negative for $\Delta > 0$—these regions are usually labeled as stable (cooling) and unstable (heating), and (iii) K as a function of Δ crosses zero once if $\gamma \geqslant \Omega$ (the case of free-mass GWD interferometers) and (iv) three times otherwise (the case of micromechanical oscillators in the resolved sideband limit). These properties are illustrated in Figs. 2(a) and 2(b).

Off the dark port for $\xi \neq 0$, features (i)–(iii) are lost. In this sense we refer to the dynamic backaction in a MSI operated off the dark fringe as anomalous. In particular, both K and Γ become highly asymmetric and acquire nonzero values at $\Delta = 0$ [see Figs. 2(c) and 2(d)], such that for a certain region of parameters $\Gamma|_{\Delta=0} > 0$—this is *cooling on cavity resonance*. Also optical damping can cross zero several times, acquiring additional regions of stability and instability [see the inset in Fig. 2(c)], thus allowing *other regimes of cooling and heating respectively*. Nonzero K at $\Delta = 0$ implies a shift of the mechanical frequency on resonance, although for micromechanical oscillators it is mostly negligible compared to their intrinsic mechanical frequencies. The influence of the optical losses can be estimated by the corresponding increase of $T_{\rm SR}^2$.

We note that at fixed mechanical frequency $\omega_{\rm m}$ the optical damping is proportional to the antisymmetric part of the unsymmetrized spectral density S_F of backaction noise, $\Gamma \sim S_F(\omega_{\rm m}) - S_F(-\omega_{\rm m})$ (see [2]). Since in cavity optomechanics the transformation of the Lorentzian profile of S_F into the mixture of Lorentz and Fano types is governed by the interplay between dispersive and dissipative couplings [42,46,47], one can argue that the same mechanism leads to the transformation of canonical dynamic backaction into the anomalous kind. Dynamic backaction corresponding to pure dissipative coupling in a single-mode cavity optomechanics was considered in [47], where it was shown that although both the optical spring and damping remain antisymmetric with respect to Δ (and vanish at $\Delta = 0$), damping acquires additional regions of stability and instability on either side of the cavity resonance.

The extreme case of a 100% reflective membrane in a MSI corresponds to a pure MI, i.e., reproduces the basic topology of GWDs. The coordinate x of the mechanical degree of freedom refers then to the differential motion of the end mirrors in the arms of the MI [see Fig. 1(e)]. For a GWD, being a free-mass interferometer, the effect of the optical spring is not negligible, since it transforms (almost) free test masses into mechanical oscillators with resonance frequencies lying in the GW observation band, where typically $\Omega < \gamma$. Thus, if a detuned interferometer is operated at dark fringe, Eq. (1) for $\xi = 0$ implies either $K > 0$, $\Gamma < 0$ for $\Delta > 0$, or $K < 0$, $\Gamma > 0$ for $\Delta < 0$. This means that for a single laser drive a set of canonical K and Γ is unstable in both cases.

However, a MI also exhibits anomalous dynamic backaction if operated off the dark port, violating features (ii) and (iii) of the canonical form: in the limit of a quasifree mass, $\Omega \to 0$, which is of particular interest for GWDs, Eq. (1) reduces to

$$K = \frac{4\omega_0 P_{\rm in}}{c\mathcal{L}} \frac{\Delta}{\gamma^2 + \Delta^2} \left[1 - \frac{4\gamma\gamma_{\rm m}}{\gamma^2 + \Delta^2} \right], \quad (2a)$$

$$\Gamma = -\frac{4\omega_0 P_{\rm in}}{c\mathcal{L}} \frac{\gamma\Delta}{(\gamma^2 + \Delta^2)^2} \left[1 - \frac{\gamma_{\rm m}}{\gamma} \frac{3\gamma^2 - \Delta^2}{\gamma^2 + \Delta^2} \right]. \quad (2b)$$

Both K and Γ vanish on resonance, and one can check using Eq. (1) that this feature holds for any Ω. The

[2]The sign of $\delta_{\rm m}$ alternates in the sequence of dark ports, starting with $+$ for $n = 1$. Note that shifts in both linewidth ($\gamma_{\rm m}$) and detuning ($\delta_{\rm m}$) due to offset from the dark fringe are *quadratic* in displacement.

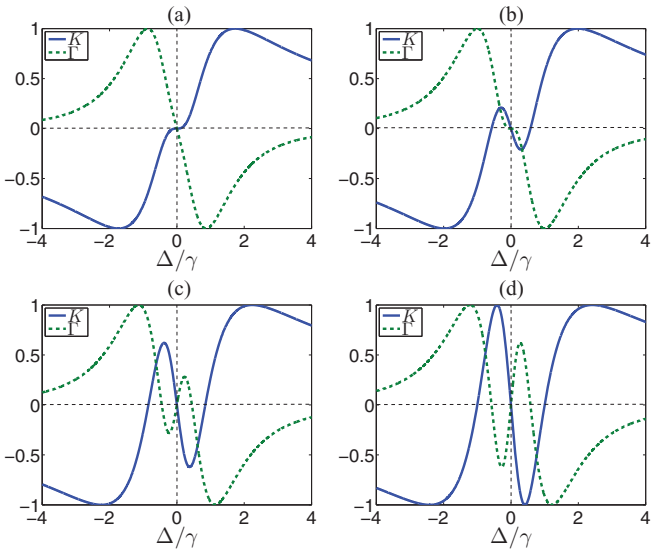

FIG. 3. (Color online) Anomalous K and Γ in a Michelson interferometer, defined by Eqs. (2a) and (2b), and normalized to their respective maximum values. (a) K acquires three zeros starting from $\gamma_m = \gamma/4$, or equivalently, $\gamma_m = \gamma_{SR}/3$. (b) Γ acquires three zeros starting from $\gamma_m = \gamma/3$ or $\gamma_m = \gamma_{SR}/2$. (c) $\gamma_m = 7\gamma/3$ or $\gamma_m = 3\gamma_{SR}/4$ and (d) $\gamma_m = \gamma/2$ or $\gamma_m = \gamma_{SR}$ demonstrate the existence of stable optical spring ($K > 0$ and $\Gamma > 0$) in a certain range of detunings for larger offsets from the dark fringe.

terms in square brackets in Eqs. (2a) and (2b) represent the deviations from canonical formulas. According to these terms, the optical spring can have three zeros at $\Delta = 0$ and $\Delta = \pm\sqrt{\gamma(4\gamma_m - \gamma)}$, if $\gamma_m > \gamma/4$. Similarly, the optical damping can also cross zero three times at $\Delta = 0$ and $\Delta = \pm\gamma\sqrt{(3\gamma_m - \gamma)/(\gamma + \gamma_m)}$, if $\gamma_m > \gamma/3$. This sequence of transformations of the canonical K and Γ, shown in Fig. 2(a), into the anomalous ones for increasing values of γ_m is illustrated in Fig. 3. Since the second-generation GWDs will be utilizing the single-photodiode homodyne readout (dc readout), when the offset from the dark port is created on purpose to transmit a small portion of the mean power to the detection port, the anomalous optical spring and damping may have an impact on the control of detectors in the detuned regime ($\Delta \neq 0$). Additionally, in realistic dual-recycled interferometers (SR *and* PR) the anomalous optical spring should be expected at even smaller ξ, since anomalies rise at $k_0\xi \sim \sqrt{T_{SR}^2 T_{PR}^2}$, where T_{PR}^2 stands for the power reflectivity of the PR mirror, compared to $k_0\xi \sim \sqrt{T_{SR}^2}$ for pure SR topologies.

Figures 3(c) and 3(d) show that for a large enough offset from the dark fringe several intersecting regions of positive and negative K and Γ appear, such that for a certain range of negative detunings both K and Γ are positive, indicating a possible stable state. An accurate analysis of the stability in terms of Routh-Hurwitz criteria indeed reveals that there exists a region of parameters where the set of K and Γ makes a stable optical spring which can be utilized for the increase of the quantum-noise-limited sensitivity of GWD topologies, such as traditional detuned-SR topology and promising intracavity topologies of optical bars [48] and optical levers [48,49].

III. CONCLUSIONS

We have shown that the dynamic backaction in interferometers operated off the dark port exhibits anomalous features as compared to the canonical type in dark-port-operated interferometers, and should be expected as a generic feature in optomechanical systems which exhibit a mixture of dispersive and dissipative couplings. In particular, in a SR MSI with a translucent micromechanical membrane, cooling and heating of the latter become possible on resonance. Additionally, as a generic feature of dissipatively coupled systems, cooling of the membrane to near the quantum ground state outside the resolved sideband regime can be in principle achieved. We have demonstrated that the scaling law—which is the cornerstone of characterization of the optomechanics of GWD topologies—is invalidated for interferometers operated off the dark port. In particular, for a large enough offset from the dark port in a MI, a stable optical spring, used for the reduction of quantum noise, becomes possible with a single laser carrier. The latter condition is important, because the canonical optical spring (on the dark port) can be stabilized only with either additional feedback and control loops or a second laser carrier [50–52], which is undesirable in experiments. Thus, the offset from the dark fringe makes a useful additional degree of freedom in shaping of the optical spring, and, in principle, may help in converting the latter into the so-called *optical inertia* [53] which allows broadband reduction of quantum noise. However, since a large offset from the dark fringe will couple mean power and technical laser noise into the detector port, certain changes in the GWD topology will be required to make use of the stable single-carrier optical spring, such as, e.g., switching to intrcavity topologies [48,49]. The anomalous aspects of backaction introduced in this paper, which will be important to estimate the consequences for next-generation GWDs, can be examined and studied on the basis of a micromechanical system. Therefore, our findings represent an example of the fruitful interplay between cavity optomechanics of micromechanical oscillators and the optomechanics of "macromechanical" oscillators as relevant to the high-precision interferometers employed for GWDs.

ACKNOWLEDGMENTS

We would like to thank Karsten Danzmann, Harald Lück, Yanbei Chen, and Stefan Hild for fruitful discussions. This work was funded by the Centre for Quantum Engineering and Space-Time Research (QUEST) at the Leibniz University Hannover, and by the European Commission through iQUOEMS. F.K. was supported by LIGO NSF Grant No. PHY-0967049 and the Russian Foundation for Basic Research Grant No. 11-02-00383-a.

APPENDIX A: PROPAGATION OF FIELDS

Consider a Michelson-Sagnac interferometer (MSI) as shown in Fig. 4 with a central beam splitter BS having amplitude reflectivity $R_{BS} = \sqrt{(1 - \delta_{BS})/2}$ and transmissivity $T_{BS} = \sqrt{(1 + \delta_{BS})/2}$, where $0 \leqslant \delta_{BS} \leqslant 1$, two steering mirrors M_1 and M_2 both having 100% reflectivity, a semitransparent membrane m with amplitude reflectivity $R_m > 0$ and

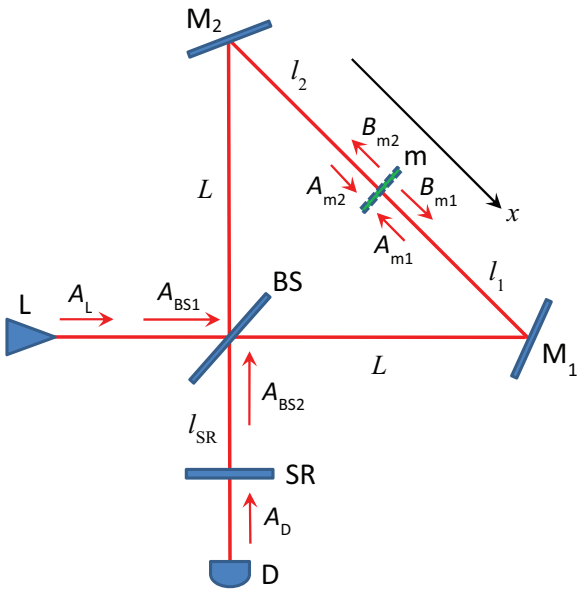

FIG. 4. (Color online) Fields in a Michelson-Sagnac interferometer.

transmissivity $T_{\rm m} > 0$, and a signal-recycling mirror SR with amplitude reflectivity $R_{\rm SR} > 0$ and transmissivity $T_{\rm SR} > 0$. The interferometer is driven by a laser L through laser port. Photons emanating through the other, detector port impinge on a detector D (homodyne or heterodyne). We denote the distance between the SR mirror and BS as $l_{\rm SR}$, arm length as L, and the distances between the folding mirrors M_1 and M_2 and membrane as $l_1 = l - \delta l/2$ and $l_2 = l + \delta l/2$, respectively. This means that $l_1 + l_2 = 2l, l_2 - l_1 = \delta l$ and the mean position of the membrane on the x axis is $\langle x\rangle = \delta l/2$. The total length of the SR-m path is $\mathcal{L} = L + l + l_{\rm SR}$.

In any spatial location inside the interferometer we decompose the electric field of the coherent, plane, and linearly polarized electromagnetic wave into the sum of a steady-state (mean) field with amplitude A_0 and carrier frequency ω_0 (wave number $k_0 = \omega_0/c$ and wavelength $\lambda_0 = 2\pi/k_0$), and slowly varying (on the scale of $1/\omega_0$) perturbation field with amplitude $a(t)$ describing vacuum noises and the contribution from the motion of the membrane,

$$A(t) = \sqrt{\frac{2\pi\hbar\omega_0}{\mathcal{A}c}}[A_0 e^{-i\omega_0 t} + a(t)e^{-i\omega_0 t}] + \text{H.c.},$$
$$a(t) = \int_{-\infty}^{+\infty} a(\omega_0+\Omega)e^{-i\Omega t}\frac{d\Omega}{2\pi}.$$

Here $\mathcal{A}$ is the area of the laser beam's cross section and c is the speed of light. Unless mentioned explicitly, we will deal with fields in the frequency domain only and omit frequency arguments for brevity.

The laser L emits a drive wave $A_{\rm L}$ with mean amplitude $A_{\rm L0}$ and optical fluctuations $a_{\rm L}$. For simplicity we assume that there are no technical fluctuations so that the laser is shot-noise limited, $[a_{\rm L}(\omega_0+\Omega), a_{\rm L}^\dagger(\omega_0+\Omega')] = 2\pi\delta(\Omega-\Omega')$. The vacuum field $A_{\rm D}$ entering through the SR mirror from the detector port has zero mean amplitude but nonzero vacuum noise $a_{\rm D}$, uncorrelated with vacuum noise from the laser port and obeying the similar commutation relation $[a_{\rm D}(\omega_0+\Omega), a_{\rm D}^\dagger(\omega_0+\Omega')] = 2\pi\delta(\Omega-\Omega')$. We unite these into vector columns of input fields $\boldsymbol{A}_{\rm in} = (A_{\rm L}, A_{\rm D})$, so that the vector of mean input fields is $\boldsymbol{A}_{\rm in0} = (A_{\rm L0}, 0)$ and the vector of perturbation fields is $\boldsymbol{a}_{\rm in} = (a_{\rm L}, a_{\rm D})$. Due to the linearity of the system input fields can be propagated throughout the interferometer as independent Fourier components.

Consider first the case without SRM and with a fixed membrane. The latter condition allows us to treat mean and perturbation fields on equal footing. Input fields (in this case coinciding with the fields incident on the beam splitter) linearly transform into the output fields: $\boldsymbol{A}_{\rm out} = \mathbb{M}_{\rm BS}^T\mathbb{P}_L\mathbb{P}_l\mathbb{M}_{\rm m}\mathbb{P}_l\mathbb{P}_L\mathbb{M}_{\rm BS}\boldsymbol{A}_{\rm in} \equiv \mathbb{M}_{\rm MS}\boldsymbol{A}_{\rm in}$. Here

$$\mathbb{M}_{\rm BS} = \begin{pmatrix} T_{\rm BS} & -R_{\rm BS} \\ R_{\rm BS} & T_{\rm BS}\end{pmatrix}, \quad \mathbb{M}_{\rm m} = \begin{pmatrix} -R_{\rm m} & T_{\rm m} \\ T_{\rm m} & R_{\rm m}\end{pmatrix} \tag{A1}$$

are the transformation matrices of beam splitter and membrane, both chosen in real form (this is always possible due to the Stokes relations), and

$$\mathbb{P}_L = \begin{pmatrix} e^{ikL} & 0 \\ 0 & e^{ikL}\end{pmatrix}, \quad \mathbb{P}_l = \begin{pmatrix} e^{ikl_1} & 0 \\ 0 & e^{ikl_2}\end{pmatrix}$$

are the propagation matrices comprised of the phase shifts along the horizontal and vertical arms (of length L) and diagonal half arms (of lengths $l_{1,2}$). For mean fields one should apply the substitution $k = k_0$ and for perturbation fields $k = k_0 + K = k_0 + \Omega/c$. The matrix $\mathbb{M}_{\rm MS}$ thus represents the transformation matrix of a nonrecycled MSI,

$$\mathbb{M}_{\rm MS} = e^{2ik(L+l)}\begin{pmatrix} \rho_1 & \tau \\ \tau & \rho_2\end{pmatrix},$$

with

$$\rho_1 = R_{\rm m}\left(R_{\rm BS}^2 e^{ik\delta l} - T_{\rm BS}^2 e^{-ik\delta l}\right) + 2T_{\rm m}R_{\rm BS}T_{\rm BS},$$
$$\rho_2 = R_{\rm m}\left(T_{\rm BS}^2 e^{ik\delta l} - R_{\rm BS}^2 e^{-ik\delta l}\right) - 2T_{\rm m}R_{\rm BS}T_{\rm BS},$$
$$\tau = R_{\rm m}R_{\rm BS}T_{\rm BS}(e^{ik\delta l} + e^{-ik\delta l}) + T_{\rm m}\left(T_{\rm BS}^2 - R_{\rm BS}^2\right).$$

In Sec. II we denoted $\rho \equiv \rho_2$. Physically ρ_1 is the reflectivity of the input laser field back into the laser port, $\rho_2 = -\rho_1^*$ is the reflectivity of the input vacuum field back into the detector port, and τ is the transmissivity of the laser field into the detector port and the vacuum field into the laser port. One can check that the matrix $\mathbb{M}_{\rm MS}$ is unitary; thus a *nonrecycled MSI can be described as an effective mirror with reflectivity and transmissivity depending on the membrane position* via δl, as stated in Sec. II and discussed already in [46]. The dark port (dark fringe) condition for the interferometer is achieved when the cross transmittance between input and output ports vanishes (in particular, no mean power leaks into the detector port), corresponding to $\tau = 0$, or explicitly

$$\cos k_0\delta l = -\frac{T_{\rm m}}{R_{\rm m}}\frac{\delta_{\rm BS}}{\sqrt{1-\delta_{\rm BS}^2}}. \tag{A2}$$

In the case of a symmetric beam splitter ($\delta_{\rm BS} = 0$) this is satisfied for $\delta l = n\lambda_0/4$ and odd n.[3]

[3]For other choices of transfer matrices (A1) the dark port condition will correspond to a different δl but this is insignificant, since the absolute phase does not matter.

If the SRM is inserted then the outgoing field in the SR port is reflected back, such that the ingoing fields incident on the beam splitter are defined by the equation

$$\boldsymbol{A}_{\rm BS} = \mathbb{P}_{\rm R}\mathbb{T}_{\rm R}\boldsymbol{A}_{\rm in} + \mathbb{P}_{\rm R}\mathbb{R}_{\rm R}\mathbb{P}_{\rm R}\mathbb{M}_{\rm MS}\boldsymbol{A}_{\rm BS}. \tag{A3}$$

Here $\boldsymbol{A}_{\rm BS} = (A_{\rm BS1}, A_{\rm BS2})$ is the vector column of ingoing beam splitter fields (see Fig. 4), $\mathbb{R}_{\rm R} = {\rm diag}(0, R_{\rm SR})$ with zero standing for the absence of the power-recycling mirror in the laser port, $\mathbb{P}_{\rm R} = {\rm diag}(1, e^{ikl_{\rm SR}})$ is the propagation matrix in the BS-SR path, and $\mathbb{T}_{\rm R} = {\rm diag}(1, T_{\rm SR})$. Thus the first summand on the right-hand side of Eq. (A3) stands for the input fields directly incident on the beam splitter, while the second summand corresponds to a single round trip along the interferometer with reflection from the SRM. Solution of this equation yields

$$\boldsymbol{A}_{\rm BS} = (\mathbb{I} - \mathbb{P}_{\rm R}\mathbb{R}_{\rm R}\mathbb{P}_{\rm R}\mathbb{M}_{\rm MS})^{-1}\mathbb{P}_{\rm R}\mathbb{T}_{\rm R}\boldsymbol{A}_{\rm in}, \tag{A4}$$

where $\mathbb{I}$ is the 2×2 unity matrix. We denote the inverse matrix in this solution as $\mathbb{K}_{\rm MSR}$,

$$\mathbb{K}_{\rm MSR} = \frac{1}{\mathcal{D}}\begin{pmatrix} \mathcal{D} & 0 \\ R_{\rm SR}\tau e^{2ik\mathcal{L}} & 1 \end{pmatrix}, \quad \mathcal{D} = 1 - R_{\rm SR}\rho_2 e^{2ik\mathcal{L}}.$$

This tells us that *the MSI with a SRM makes an effective Fabry-Pérot cavity* with associated resonance factor $1/\mathcal{D}$, as stated in Sec. II. The matrix element $\mathbb{K}^{(2,2)}_{\rm MSR}$ describes a resonant amplification of the input vacuum field inside the cavity, while $\mathbb{K}^{(2,1)}_{\rm MSR}$ corresponds to the laser field being partially transmitted into the SR port (hence the proportionality to τ) and also enhanced inside the cavity. In the ideal dark-port regime cross transmittance is suppressed, all the laser field is reflected back into the laser port, and only the vacuum field from the detector port resonates inside the cavity.

Note that the effective detuning of the laser carrier from cavity resonance(s) is not solely defined by the corresponding shift in frequency (or cavity length), in contrast to the ordinary Fabry-Pérot cavity. Assume that $\arg\rho_2 = \phi_{\rm DP} + \delta\phi$, where $\phi_{\rm DP} = \arg\rho_2|_{\rm dark\ port}$ and $\delta\phi$ is the deviation from it due to offset from the dark fringe via membrane positioning, and $2k\mathcal{L} + \phi_{\rm DP} = 2\pi N + 2\delta_k\mathcal{L}$, N is integer, and $\delta_k\mathcal{L} \ll 1$. Then one can rewrite the inverse resonance factor as

$$\mathcal{D} = 1 - R_{\rm SR}|\rho_2|e^{2ik\mathcal{L}+i\arg\rho_2} = 1 - R_{\rm SR}|\rho_2|e^{2i\Delta\mathcal{L}/c},$$

such that the full detuning

$$\Delta = \delta + \frac{c}{2\mathcal{L}}\delta\phi$$

is the sum of the "conventional" detuning $\delta = c\delta_k$ of the carrier frequency from the cavity resonance at the dark port, and an additional detuning $c\delta\phi/(2\mathcal{L})$ corresponding to the offset from the latter.

The narrowband limit is achieved when both the SRM and compound "interferometer" mirror possess high reflectivity, $1 - R_{\rm SR} \approx T^2_{\rm SR}/2 \ll 1$ and $1 - |\rho_2| \approx \tau^2/2 \ll 1$. The half-linewidth of the cavity is then

$$\gamma = \frac{1 - R_{\rm SR}|\rho_2|}{2\mathcal{L}/c} \approx \frac{cT^2_{\rm SR}}{4\mathcal{L}} + \frac{c\tau^2}{4\mathcal{L}}.$$

Therefore, the total cavity linewidth accounts for finite SRM transmittance and finite transmittance of the interferometer operated off the dark port; since $\tau = \tau(\delta l)$, the latter contribution describes modulation of the linewidth by the motion of the membrane, thus implementing dissipative coupling in the effective cavity, as stated in Sec. II and discussed already in [46].

APPENDIX B: STOCHASTIC BACKACTION

In order to determine the radiation pressure force acting on the membrane we need to determine the fields on the membrane surfaces. Ingoing fields on the beam splitter (A4) propagate along the arms and transform into the fields incident on the membrane $(A_{\rm m1}, A_{\rm m2}) = \boldsymbol{A}_{\rm m} = \mathbb{P}_l\mathbb{P}_L\mathbb{M}_{\rm BS}\boldsymbol{A}_{\rm BS}$ and reflected from it $(B_{\rm m1}, B_{\rm m2}) = \boldsymbol{B}_{\rm m} = \mathbb{M}_{\rm m}\boldsymbol{A}_{\rm m}$ (see Fig. 4). In terms of the input fields

$$\boldsymbol{A}_{\rm m} = \mathbb{M}_A\boldsymbol{A}_{\rm in};\ \mathbb{M}_A = \mathbb{P}_l\mathbb{P}_L\mathbb{M}_{\rm BS}\mathbb{K}_{\rm MSR}\mathbb{P}_{\rm R}\mathbb{T}_{\rm R}, \tag{B1a}$$

$$\boldsymbol{B}_{\rm m} = \mathbb{M}_B\boldsymbol{A}_{\rm in};\ \mathbb{M}_B = \mathbb{M}_{\rm m}\mathbb{P}_l\mathbb{P}_L\mathbb{M}_{\rm BS}\mathbb{K}_{\rm MSR}\mathbb{P}_{\rm R}\mathbb{T}_{\rm R}. \tag{B1b}$$

The components of the matrix $\mathbb{M}_A$ are

$$\begin{aligned}
\mathbb{M}^{(1,1)}_A &= \mathcal{D}^{-1}[T_{\rm BS}(1 - R_{\rm m}R_{\rm SR}e^{2ik(\mathcal{L}+\delta l/2)}) \\
&\quad + R_{\rm BS}T_{\rm m}R_{\rm SR}e^{2ik\mathcal{L}}]e^{ik(L+l-\delta l/2)}, \\
\mathbb{M}^{(1,2)}_A &= -\mathcal{D}^{-1}T_{\rm SR}R_{\rm BS}e^{ik(\mathcal{L}-\delta l/2)}, \\
\mathbb{M}^{(2,1)}_A &= \mathcal{D}^{-1}[R_{\rm BS}(1 + R_{\rm m}R_{\rm SR}e^{2ik(\mathcal{L}-\delta l/2)}) \\
&\quad + T_{\rm BS}T_{\rm m}R_{\rm SR}e^{2ik\mathcal{L}}]e^{ik(L+l+\delta l/2)}, \\
\mathbb{M}^{(2,2)}_A &= \mathcal{D}^{-1}T_{\rm SR}T_{\rm BS}e^{ik(\mathcal{L}+\delta l/2)},
\end{aligned}$$

and of the matrix $\mathbb{M}_B$

$$\begin{aligned}
\mathbb{M}^{(1,1)}_B &= \mathcal{D}^{-1}[-T_{\rm BS}(R_{\rm m} - R_{\rm SR}e^{2ik(\mathcal{L}+\delta l/2)}) \\
&\quad + T_{\rm m}R_{\rm BS}e^{ik\delta l}]e^{ik(L+l-\delta l/2)}, \\
\mathbb{M}^{(1,2)}_B &= \mathcal{D}^{-1}T_{\rm SR}(R_{\rm BS}R_{\rm m} + T_{\rm m}T_{\rm BS}e^{ik\delta l})e^{ik(\mathcal{L}-\delta l/2)}, \\
\mathbb{M}^{(2,1)}_B &= \mathcal{D}^{-1}[R_{\rm BS}(R_{\rm m} + R_{\rm SR}e^{2ik(\mathcal{L}-\delta l/2)}) \\
&\quad + T_{\rm m}T_{\rm BS}e^{-ik\delta l}]e^{ik(L+l+\delta l/2)}, \\
\mathbb{M}^{(2,2)}_B &= \mathcal{D}^{-1}T_{\rm SR}(T_{\rm BS}R_{\rm m} - T_{\rm m}R_{\rm BS}e^{-ik\delta l})e^{ik(\mathcal{L}+\delta l/2)}.
\end{aligned}$$

We denote these transfer matrices separately for the mean fields as $\mathbb{M}_{A_0} = \mathbb{M}_A|_{k=k_0}$, $\mathbb{M}_{B_0} = \mathbb{M}_B|_{k=k_0}$ and for the perturbation fields as $\mathbb{M}_a(\Omega) = \mathbb{M}_A|_{k=k_0+K}$, $\mathbb{M}_b(\Omega) = \mathbb{M}_B|_{k=k_0+K}$.

The radiation pressure force exerted on the membrane is then given by

$$F(t) = -\frac{\mathcal{A}}{4\pi}\left\langle A^2_{\rm m1}(t) + B^2_{\rm m1}(t) - A^2_{\rm m2}(t) - B^2_{\rm m2}(t)\right\rangle, \tag{B2}$$

where averaging is performed over the period of electromagnetic oscillations. Ignoring the dc contribution and linearizing with respect to perturbation terms, the spectrum of the force

reads

$$F_{\rm BA}(\Omega) = 2\hbar k_0 R_{\rm m} \boldsymbol{A}^{*T}_{\rm in0} \mathbb{M}^{*T}_{A_0} \mathbb{M}_b(\Omega) \boldsymbol{a}_{\rm in}(\omega_0+\Omega) + 2\hbar k_0 R_{\rm m} \boldsymbol{A}^{T}_{\rm in0} \mathbb{M}^{T}_{A_0} \mathbb{M}^{*}_b(-\Omega) \boldsymbol{a}^{\dagger}_{\rm in}(\omega_0-\Omega).$$

This is the radiation pressure noise, also addressed as backaction noise or stochastic back-action, i.e., the time-varying radiation pressure that is solely caused by the fluctuations of optical fields. The unsymmetrized spectral density of stationary backaction noise is computed from the equation $2\pi\delta(\Omega-\Omega')S_F(\Omega') = \langle 0|F_{\rm BA}(\Omega)F^{\dagger}_{\rm BA}(\Omega')|0\rangle$, yielding

$$S_F(\Omega) = \frac{4\hbar k_0}{c}\frac{R_{\rm m}^2 P_{\rm in}}{|\mathcal{D}_0\mathcal{D}(\Omega)|^2}\left\{|\mathfrak{L}(\Omega)|^2 + T_{\rm SR}^2\,|\mathfrak{D}(\Omega)|^2\right\}, \quad \text{(B3)}$$

$$\mathfrak{L}(\Omega) = \alpha_1\left(1+R_{\rm SR}^2 e^{2iK\mathcal{L}}\right) + \alpha_2 R_{\rm SR} e^{2i(k_0+K)\mathcal{L}} + \alpha_2^* R_{\rm SR} e^{-2ik_0\mathcal{L}},$$

$$\mathfrak{D}(\Omega) = \beta_1 + \beta_2 R_{\rm SR} e^{-2ik_0\mathcal{L}},$$

$$\alpha_1 = T_{\rm m}R_{\rm BS}T_{\rm BS}(e^{ik\delta l}+e^{-ik\delta l}) - R_{\rm m}\left(T_{\rm BS}^2 - R_{\rm BS}^2\right),$$

$$\alpha_2 = T_{\rm BS}^2 e^{ik\delta l} + R_{\rm BS}^2 e^{-ik\delta l},$$

$$\beta_1 = T_{\rm m}\left(T_{\rm BS}^2 e^{ik\delta l} - R_{\rm BS}^2 e^{-ik\delta l}\right) + 2R_{\rm m}R_{\rm BS}T_{\rm BS},$$

$$\beta_2 = R_{\rm BS}T_{\rm BS}(e^{ik\delta l} - e^{-ik\delta l}).$$

Here $P_{\rm in} = \hbar\omega_0|A_{\rm L0}|^2$ is the input laser power, $\mathcal{D}_0 = \mathcal{D}|_{k=k_0}$ is the resonant multiplier for mean fields, and $\mathcal{D}(\Omega) = \mathcal{D}|_{k=k_0+K}$ is the resonant multiplier for perturbation fields.

The factors $\mathfrak{L}$ and $\mathfrak{D}$ in Eq. (B3) describe contributions of vacuum noises from the laser ($a_{\rm L}$) and detector ports ($a_{\rm D}$), respectively. The former defines the Fano-line profile in the shape of S_F due to interference of input and intracavity laser fields on the membrane, and is identified with the emergence of dissipative coupling in cavity optomechanics [42,46,47]. The latter, vanishing for the 100% reflective SRM [46], describes a Lorentzian profile of the intracavity vacuum field from the detector port, and is identified with dispersive coupling in cavity optomechanics. Therefore, the spectral density of backaction noise in the general case is the mixture of Fano and Lorentz resonances, as mentioned in Sec. II. Plots of normalized $S_F(\Omega)$ are presented in Figs. 5(a) and 5(b) for $T_{\rm SR} = 0$ and $T_{\rm SR} \neq 0$, respectively.

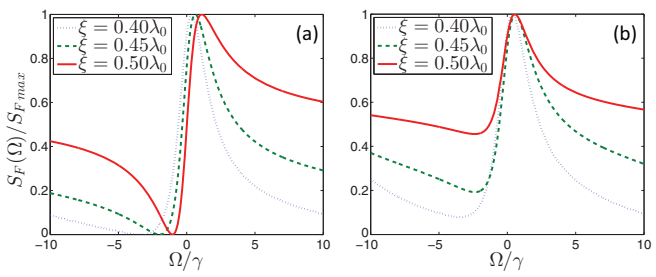

FIG. 5. (Color online) Normalized (nonsymmetrized) spectral densities of backaction noise for different membrane positions $\xi = \delta l - \delta l_{\rm DP}$ where $\delta l_{\rm DP}$ is defined by Eq. (A2). For better visualization we choose membrane power reflectivity $R_{\rm m}^2 = 0.3$, beam splitter asymmetry $\delta_{\rm BS} = -0.3$, and detuning $\Delta = 0$. (a) $R_{\rm SR}^2 = 1$. (b) $R_{\rm SR}^2 = 0.7$.

APPENDIX C: DYNAMIC BACKACTION

Consider now a movable membrane with position operator $x_{\rm m}(t)$ with a corresponding Fourier-transformed operator $x_{\rm m}(\Omega)$. According to perturbation theory the fields on the membrane surfaces will have contributions of zeroth and first order in the mechanical displacement. One finds $\boldsymbol{B}_{\rm m0} = \mathbb{M}_{\rm m}\boldsymbol{A}_{\rm m0}$ and $\boldsymbol{b}_{\rm m} = \mathbb{M}_{\rm m}\boldsymbol{a}_{\rm m} + 2ik_0x_{\rm m}R_{\rm m}\boldsymbol{A}_{\rm m0}$. Thus the perturbation fields now contain both optical noises and the displacement of the membrane. Since the treatment of mean fields remains unchanged, we consider only the perturbation terms. The ingoing fields on the beam splitter are defined by the equation $\boldsymbol{a}_{\rm BS} = \mathbb{P}_{\rm R}\mathbb{T}_{\rm R}\boldsymbol{a}_{\rm in} + \mathbb{P}_{\rm R}\mathbb{R}_{\rm R}\mathbb{P}_{\rm R}\mathbb{M}_{\rm MS}\boldsymbol{a}_{\rm BS} + \mathbb{P}_{\rm R}\mathbb{R}_{\rm R}\mathbb{P}_{\rm R}\mathbb{M}^{T}_{\rm BS}\mathbb{P}_L\mathbb{P}_l\,2ik_0x_{\rm m}(\Omega)R_{\rm m}\boldsymbol{A}_{\rm m0}$, with the solution $\boldsymbol{a}_{\rm BS} = \mathbb{K}_{\rm MSR}\mathbb{P}_{\rm R}\mathbb{T}_{\rm R}\boldsymbol{a}_{\rm in} + 2ik_0x_{\rm m}\mathbb{K}_{\rm MSR}\mathbb{P}_{\rm R}\mathbb{R}_{\rm R}\mathbb{P}_{\rm R}\mathbb{M}^{T}_{\rm BS}\mathbb{P}_L\mathbb{P}_l R_{\rm m}\boldsymbol{A}_{\rm m0}$. Thus the incident and reflected fields on the membrane surfaces are

$$\boldsymbol{a}_{\rm m} = \mathbb{M}_a\boldsymbol{a}_{\rm in} + 2ik_0x_{\rm m}\mathbb{M}_{ax}\boldsymbol{A}_{\rm m0}, \quad \text{(C1a)}$$

$$\boldsymbol{b}_{\rm m} = \mathbb{M}_b\boldsymbol{a}_{\rm in} + 2ik_0x_{\rm m}(R_{\rm m}\mathbb{I} + \mathbb{M}_{\rm m}\mathbb{M}_{ax})\boldsymbol{A}_{\rm m0}. \quad \text{(C1b)}$$

The components of the matrix

$$\mathbb{M}_{ax} = \mathbb{P}_l\mathbb{P}_L\mathbb{M}_{\rm BS}\mathbb{K}_{\rm MSR}\mathbb{P}_{\rm R}\mathbb{R}_{\rm R}\mathbb{P}_{\rm R}\mathbb{M}^{T}_{\rm BS}\mathbb{P}_L\mathbb{P}_l R_{\rm m}$$

are

$$\mathbb{M}^{(1,1)}_{ax} = \mathcal{D}^{-1}R_{\rm m}R_{\rm BS}^2R_{\rm SR}e^{2ik(\mathcal{L}-\delta l/2)},$$

$$\mathbb{M}^{(2,2)}_{ax} = \mathcal{D}^{-1}R_{\rm m}T_{\rm BS}^2R_{\rm SR}e^{2ik(\mathcal{L}+\delta l/2)},$$

$$\mathbb{M}^{(1,2)}_{ax} = \mathbb{M}^{(2,1)}_{ax} = -\mathcal{D}^{-1}R_{\rm m}R_{\rm BS}T_{\rm BS}R_{\rm SR}e^{2ik\mathcal{L}}.$$

Substituting the mean fields from Eqs. (B1a) and (B1b) and the perturbation fields (C1a) and (C1b) into Eq. (B2), ignoring the dc part and linearizing with respect to perturbation terms, one ends up with $F(\Omega) = F_{\rm BA}(\Omega) + F_x(\Omega)$. Here $F_{\rm BA}$ is the radiation pressure noise considered in Appendix B, and $F_x(\Omega) = -\mathcal{K}(\Omega)x_{\rm m}(\Omega)$ is the ponderomotive force, i.e., the dynamical part of the radiation pressure force caused by the motion of the membrane. The coefficient $\mathcal{K}(\Omega)$ modifies the dynamics of the membrane, and therefore represents the dynamic backaction,

$$\mathcal{K}(\Omega) = \frac{2ik_0}{c}R_{\rm m}P_{\rm in}[\mathbb{K}_{(1,1)}(\Omega) - \mathbb{K}^{*}_{(1,1)}(-\Omega)],$$

$$\mathbb{K}(\Omega) = \mathbb{M}^{*T}_{B_0}\left[\sigma_3 - 2\mathbb{M}_{ax}(\Omega)\right]\mathbb{M}_{A_0},$$

with $\sigma_3 = {\rm diag}(1,-1)$. If one denotes $K(\Omega) \equiv {\rm Re}[\mathcal{K}(\Omega)]$ and $\Gamma(\Omega) \equiv -\frac{1}{2}\,{\rm Im}[\mathcal{K}(\Omega)]/\Omega$, then the corresponding shifts of the square of intrinsic mechanical frequency and damping rate are equal to K/m and Γ/m.[4] After applying simplifying conditions described in Sec. II, one ends up with Eq. (1) for $\mathcal{K}$ presented there.

[4]Assuming that the equation of motion of the membrane is of the following form: $\ddot{x} + 2\gamma_{\rm m}\dot{x} + \omega_{\rm m}^2 x = F(t)/m$.

[1] V. B. Braginsky and F. Ya. Khalili, *Quantum Measurement* (Cambridge University Press, Cambridge, 1992).
[2] A. A. Clerk *et al*., Rev. Mod. Phys. **82**, 1155 (2010).
[3] S. L. Danilishin and F. Ya. Khalili, Living Rev. Relativ. **15**, 5 (2012).
[4] M. Aspelmeyer, T. J. Kippenberg, and F. Marquardt, arXiv:1303.0733 [cond-mat.mes-hall].
[5] Y. Chen, arXiv:1302.1924 [quant-ph].
[6] C. M. Caves, Phys. Rev. D **23**, 1693 (1981).
[7] V. B. Braginsky, Sov. Phys. JETP **26**, 831 (1968).
[8] V. B. Braginsky and Yu. I. Vorontsov, Sov. Phys. Usp. **17**, 644 (1975).
[9] V. B. Braginsky, Yu. I. Vorontsov, and F. Ya. Khalili, JETP Lett. **27**, 276 (1978).
[10] K. W. Murch *et al*., Nat. Phys. **4**, 561 (2008).
[11] T. P. Purdy, R. W. Peterson, and C. A. Regal, Science **339**, 801 (2013).
[12] D. W. C. Brooks *et al*., Nature (London) **488**, 476 (2012).
[13] A. H. Safavi-Naeini *et al*., arXiv:1302.6179 [quant-ph].
[14] V. B. Braginsky and A. B. Manukin, Sov. Phys. JETP **25**, 653 (1967).
[15] V. B. Braginsky, A. B. Manukin, and M. Yu. Tikhonov, Sov. Phys. JETP **31**, 829 (1970).
[16] I. Wilson-Rae, N. Nooshi, W. Zwerger, and T. J. Kippenberg, Phys. Rev. Lett. **99**, 093901 (2007).
[17] F. Marquardt, J. P. Chen, A. A. Clerk, and S. M. Girvin, Phys. Rev. Lett. **99**, 093902 (2007).
[18] P. F. Cohadon, A. Heidmann, and M. Pinard, Phys. Rev. Lett. **83**, 3174 (1999).
[19] C. H. Metzger and K. Karrai, Nature (London) **432**, 1002 (2004).
[20] O. Arcizet *et al*., Nature (London) **444**, 71 (2006).
[21] S. Gigan *et al*., Nature (London) **444**, 67 (2006).
[22] C. A. Regal, J. D. Teufel, and K. W. Lehnert, Nat. Phys. **4**, 555 (2008).
[23] J. D. Thompson *et al*., Nature (London) **452**, 72 (2008).
[24] S. Gröblacher *et al*., Nat. Phys. **5**, 485 (2009).
[25] T. Rocheleau *et al*., Nature (London) **463**, 72 (2010).
[26] R. Riviere, S. Deleglise, S. Weis, E. Gavartin, O. Arcizet, A. Schliesser, and T. J. Kippenberg, Phys. Rev. A **83**, 063835 (2011).
[27] J. D. Teufel *et al*., Nature (London) **475**, 359 (2011).
[28] J. Chan *et al*., Nature (London) **478**, 89 (2011).
[29] T. Corbitt, D. Ottaway, E. Innerhofer, J. Pelc, and N. Mavalvala, Phys. Rev. A **74**, 021802(R) (2006).
[30] T. Corbitt, Y. Chen, E. Innerhofer, H. Muller-Ebhardt, D. Ottaway, H. Rehbein, D. Sigg, S. Whitcomb, C. Wipf, and N. Mavalvala, Phys. Rev. Lett. **98**, 150802 (2007).
[31] D. E. McClelland *et al*., Laser Photon. Rev. **5**, 677 (2011).
[32] B. J. Meers, Phys. Rev. D **38**, 2317 (1988).
[33] A. Buonanno and Y. Chen, Phys. Rev. D **67**, 062002 (2003).
[34] K. Yamamoto, D. Friedrich, T. Westphal, S. Goßler, K. Danzmann, K. Somiya, S. L. Danilishin, and R. Schnabel, Phys. Rev. A **81**, 033849 (2010).
[35] D. Friedrich *et al*., New J. Phys. **13**, 93017 (2011).
[36] V. B. Braginsky, M. L. Gorodetsky, and F. Ya. Khalili, Phys. Lett. A **232**, 340 (1997).
[37] F. Ya. Khalili, Phys. Lett. A **288**, 251 (2001).
[38] M. Rakhmanov, Ph.D. thesis, California Institute of Technology, 2000.
[39] A. Buonanno and Y. Chen, Phys. Rev. D **65**, 042001 (2002).
[40] V. I. Lazebny and S. P. Vyatchanin, Phys. Lett. A **344**, 7 (2005).
[41] F. Ya. Khalili, V. I. Lazebny, and S. P. Vyatchanin, Phys. Rev. D **73**, 062002 (2006).
[42] F. Elste, S. M. Girvin, and A. A. Clerk, Phys. Rev. Lett. **102**, 207209 (2009).
[43] M. Li, W. H. P. Pernice, and H. X. Tang, Phys. Rev. Lett. **103**, 223901 (2009).
[44] S. Huang and G. S. Agarwal, Phys. Rev. A **82**, 033811 (2010).
[45] S. Huang and G. S. Agarwal, Phys. Rev. A **81**, 053810 (2010).
[46] A. Xuereb, R. Schnabel, and K. Hammerer, Phys. Rev. Lett. **107**, 213604 (2011).
[47] T. Weiss, C. Bruder, and A. Nunnenkamp, New J. Phys. **15**, 045017 (2013).
[48] F. Ya. Khalili, Phys. Lett. A **317**, 169 (2003).
[49] S. L. Danilishin and F. Ya. Khalili, Phys. Rev. D **73**, 022002 (2006).
[50] H. Rehbein, H. Muller-Ebhardt, K. Somiya, S. L. Danilishin, R. Schnabel, K. Danzmann, and Y. Chen, Phys. Rev. D **78**, 062003 (2008).
[51] A. A. Rakhubovsky, S. Hild, and S. P. Vyatchanin, Phys. Rev. D **84**, 062002 (2011).
[52] A. Rakhubovsky and S. Vyatchanin, Phys. Lett. A **376**, 1405 (2012).
[53] F. Khalili, S. Danilishin, H. Muller-Ebhardt, H. Miao, Y. Chen, and C. Zhao, Phys. Rev. D **83**, 062003 (2011).